Mixing-induced *CP* asymmetry in $B \to K^* \gamma$ decays with perturbative QCD approach

M. Matsumori[1,*] and A. I. Sanda[1,2,†]

[1]*Department of Physics, Nagoya University, Chikusa-ku Furo-cho, Nagoya 464-8602, Japan*

[2]*Kanazawa University, 3-27-1 Rokukakubashi Kanazawa-ku, Yokohama-shi, Yokohama, Japan*

(Received 14 December 2005; published 21 June 2006)

The mixing-induced *CP* asymmetries in $B \to K^* \gamma \to K_S \pi^0 \gamma$ and $B \to K^* \gamma \to K_L \pi^0 \gamma$ are expected to be small within the standard model. So they are among the most promising decay modes to test the standard model. In this paper, we compute the mixing-induced *CP* asymmetries in these decay modes, within the framework of the standard model, using perturbative QCD, and our conclusion is $S_{K_S \pi^0 \gamma} = -S_{K_L \pi^0 \gamma} = -(3.5 \pm 1.7) \times 10^{-2}$.

DOI: 10.1103/PhysRevD.73.114022 PACS numbers: 13.20.He, 12.38.Bx, 13.40.Gp, 13.40.Hq

I. INTRODUCTION

The standard model (SM), which includes the Kobayashi-Maskawa (KM) scheme for *CP* violation [1], is being tested by determining the three sides and three angles of the unitary triangle. The observations of the *CP* asymmetries in $B \to J/\psi K_S$ [2,3], $B \to \pi\pi$ [4,5], and $B \to DK$ [6,7] decays show that a major contribution to *CP* violation comes from the KM scheme. We know that the KM scheme is not the whole story. Baryogenesis cannot be explained by this scheme. To understand this, we must search for new physics. It is therefore important to consider all possible *CP* violating phenomena.

Among many B meson decay modes, the radiative decay $B \to K^* \gamma$ attracted much attention because it is a flavor-changing-neutral-current process, which occurs only through quantum corrections. So it is expected to be sensitive to the physics beyond the SM. This decay has been seen, and first experimental results on *CP* asymmetry and isospin breaking effects have been investigated [8,9]. This has also been investigated within the framework of perturbative QCD (pQCD) [10,11]. We expect the experimental situation to improve in the near future.

There is a good reason why the mixing-induced *CP* asymmetry in $B \to K^* \gamma$ is expected to be small within the SM. If B^0 and $\bar{B}^0$ mesons can decay into a common final state f, the mixing-induced *CP* asymmetry is generated by the interference between $\bar{B}^0 \to f$ and $\bar{B}^0 \to B^0 \to f$ decay amplitudes as shown in Fig. 1. For $B \to K^* \gamma$ decay, the candidates for f are $K_S \pi^0 \gamma$ and $K_L \pi^0 \gamma$. Throughout this paper, whenever we write $B^0 \to K_{(S,L)} \pi^0 \gamma$, we mean $K_{(S,L)} \pi^0 \gamma$ to come from $B^0 \to K^{*0} \gamma \to K_{(S,L)} \pi^0 \gamma$. The continuum background $K_{(S,L)} \pi^0$ which is not from the K^{*0} decay can be subtracted. While a detailed experimental study is necessary to understand the error on the asymmetry coming from this background, we guess that the error is much smaller than the theoretical error included in our result. The $\bar{B}^0$ meson dominantly decays into a photon with left-handed chirality as shown in Fig. 2(a), because the chirality is automatically determined by the vertex structure. In order to generate the asymmetry, the amplitudes representing the two paths shown in Fig. 1 must interfere. Both B^0 and $\bar{B}^0$ must decay to the same final state f. However, the B^0 meson dominantly decays into a photon with right-handed chirality as shown in Fig. 2(b). That is, the dominant contributions of $\bar{B}^0$ and B^0 meson decays have different photon chiralities, and they cannot interfere. The amplitude which can interfere, $A(B^0 \to K_{(S,L)} \pi^0 \gamma_L)$, is suppressed by the factor of m_s/m_b compared to $A(B^0 \to K_{(S,L)} \pi^0 \gamma_R)$; thus the asymmetry which is generated by $B^0 \leftrightarrow \bar{B}^0$ mixing is suppressed by m_s/m_b [12]. If the experimental data show a large mixing-induced *CP* asymmetry, much larger than 10%, for example, it directly indicates that there exist a new physics beyond the SM. So we expect that the mixing-induced *CP* asymmetry in the $B \to K^* \gamma$ decay mode is a crucial decay mode to test the SM. The experimental data for mixing-induced *CP* asymmetry in $B \to K^* \gamma$ are given by Belle and *BABAR* as follows [13–15]:

$$S^{\rm ex}_{K^*\gamma \to K_S \pi^0 \gamma} = \begin{cases} -0.79^{+0.63}_{-0.50} \pm 0.10 & [\text{Belle}], \\ -0.21 \pm 0.40 \pm 0.05 & [\textit{BABAR}]. \end{cases}$$

This paper is organized as follows: in Sec. II, we want to review the B meson decay and mixing-induced *CP* asymmetry, and in Sec. III, we show decay amplitudes for $B \to K^* \gamma$ decay which is classified into left-handed or right-handed photon chiralities. We show the numerical results

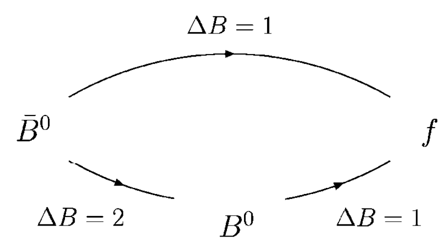

FIG. 1. The mixing-induced *CP* asymmetry is caused by the interference between $\bar{B}^0 \to f$ and $\bar{B}^0 \to B^0 \to f$ decay amplitudes.

*Electronic address: mika@eken.phys.nagoya-u.ac.jp

†Electronic address: sanda@eken.phys.nagoya-u.ac.jp

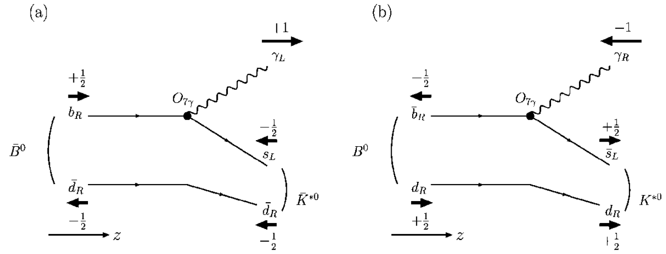

FIG. 2. Figures (a) and (b) show the major decay modes and the helicity configurations of the radiative decays of b_R, and $\bar{b}_R$, respectively.

in Sec. IV, and in Sec. V we present our conclusion on the mixing-induced CP asymmetry in $B \to K^*\gamma$ decay.

II. B MESON DECAY

A. Mixing-induced CP asymmetry

Here we want to review the mixing-induced CP asymmetry in the neutral B meson decay system [16–18]. There are two neutral B mesons, B^0 and $\bar{B}^0$, and if we turn off the weak interaction, B^0 and $\bar{B}^0$ mesons are independent of each other, and the transition between B^0 and $\bar{B}^0$ mesons does not occur. But if the weak interaction is once turn on, B^0 and $\bar{B}^0$ mesons change each other through the common mediated states f. The time-dependent CP asymmetry is given as follows:

$$A_{CP}(t) = \frac{\Gamma(\bar{B}^0(t) \to f) - \Gamma(B^0(t) \to f)}{\Gamma(\bar{B}^0(t) \to f) + \Gamma(B^0(t) \to f)} = A\cos\Delta Mt + S\sin\Delta Mt, \tag{2.1}$$

$$A = -\frac{1 - |\bar{\rho}|^2}{1 + |\bar{\rho}|^2}, \qquad S = \frac{2\,\mathrm{Im}[\frac{q}{p}\bar{\rho}]}{1 + |\bar{\rho}|^2}, \tag{2.2}$$

where

$$A(f) = \langle f|H_{\rm eff}|B^0\rangle, \quad \bar{A}(f) = \langle f|H_{\rm eff}|\bar{B}^0\rangle, \quad \bar{\rho} = \frac{\bar{A}(f)}{A(f)}. \tag{2.3}$$

Here S is called the mixing-induced CP asymmetry, and in the $B \to J/\psi K_S$ case, for example, $S = \sin 2\phi_1$. We can test the SM by determining the three angles from ϕ_1 to ϕ_3 by investigating the mixing-induced CP asymmetries in some decay channels.

B. Mixing-induced CP asymmetry in $B^0 \to K_S\pi^0\gamma$ and $B^0 \to K_L\pi^0\gamma$

Next we want to discuss the mixing-induced CP asymmetry in $B \to K^*\gamma$ decay. In order to examine the CP asymmetry, we have to look for the common final states between B^0 and $\bar{B}^0$ meson decays. The candidates in $B \to K^*\gamma$ decay are $B \to K_S\pi^0\gamma$ and $B \to K_L\pi^0\gamma$; K^* meson decays into K^0 and π^0, and K^0 meson goes to K_S or K_L.

The effective Hamiltonian which induces the flavor-changing $b \to s\gamma$ transition is given by [19]

$$\begin{aligned} H_{\rm eff}(\Delta B = 1) = \frac{G_F}{\sqrt{2}}\bigg[\sum_{q=u,c} V_{qb}V_{qs}^*\{C_1(\mu)O_1^{(q)}(\mu) \\ + C_2(\mu)O_2^{(q)}(\mu)\} - V_{tb}V_{ts}^*\bigg\{\sum_{i=3\sim 6} C_iO_i(\mu) \\ + C_{7\gamma}O_{7\gamma}(\mu) + C_{8g}(\mu)O_{8g}(\mu)\bigg\}\bigg] + \text{H.c.}, \end{aligned} \tag{2.4}$$

where C_i's are Wilson coefficients, and O_i's are local operators which are given by

$$\begin{aligned} O_1^{(q)} &= (\bar{s}_iq_j)_{V-A}(\bar{q}_jb_i)_{V-A}, \\ O_2^{(q)} &= (\bar{s}_iq_i)_{V-A}(\bar{q}_jb_j)_{V-A}, \\ O_3 &= (\bar{s}_ib_i)_{V-A}\sum_q(\bar{q}_jq_j)_{V-A}, \\ O_4 &= (\bar{s}_ib_j)_{V-A}\sum_q(\bar{q}_jq_i)_{V-A}, \\ O_5 &= (\bar{s}_ib_i)_{V-A}\sum_q(\bar{q}_jq_j)_{V+A}, \\ O_6 &= (\bar{s}_ib_j)_{V-A}\sum_q(\bar{q}_jq_i)_{V+A}, \\ O_{7\gamma} &= \frac{e}{4\pi^2}\bar{s}_i\sigma^{\mu\nu}(m_sP_L + m_bP_R)b_iF_{\mu\nu}, \\ O_{8g} &= \frac{g}{4\pi^2}\bar{s}_i\sigma^{\mu\nu}(m_sP_L + m_bP_R)T_{ij}^ab_jG_{\mu\nu}^a. \end{aligned} \tag{2.5}$$

Here we set $P_L^R = (1 \pm \gamma^5)/2$ and $(\bar{q}_iq_i)_{V\mp A}$ means $2\bar{q}_i\gamma^\mu P_R^Lq_i$, where i and j are color indexes.

We consider the decay amplitudes $B \to K_S\pi^0\gamma$ and $B \to K_L\pi^0\gamma$. The decay amplitude $A(B \to K_{S,L}\pi^0\gamma)$ can be extracted as follows: first the B meson decays into K^* and γ by the weak interaction. The decay amplitudes caused by $O_{7\gamma}$ operator can be expressed as

$$\begin{aligned} A_L &\equiv A(B^0 \to K^{*0}\gamma_L) \\ &= Fm_s\langle K^{*0}\gamma_L|\bar{b}\sigma^{\mu\nu}(1 + \gamma^5)sF_{\mu\nu}|B^0\rangle, \\ A_R &\equiv A(B^0 \to K^{*0}\gamma_R) \\ &= Fm_b\langle K^{*0}\gamma_R|\bar{b}\sigma^{\mu\nu}(1 - \gamma^5)sF_{\mu\nu}|B^0\rangle, \\ \bar{A}_L &\equiv A(\bar{B}^0 \to \bar{K}^{*0}\gamma_L) \\ &= F^*m_b\langle\bar{K}^{*0}\gamma_L|\bar{s}\sigma^{\mu\nu}(1 + \gamma^5)bF_{\mu\nu}|\bar{B}^0\rangle, \\ \bar{A}_R &\equiv A(\bar{B}^0 \to \bar{K}^{*0}\gamma_R) \\ &= F^*m_s\langle\bar{K}^{*0}\gamma_R|\bar{s}\sigma^{\mu\nu}(1 - \gamma^5)bF_{\mu\nu}|\bar{B}^0\rangle, \end{aligned} \tag{2.6}$$

where we set the common factor;

$$F \equiv V_{tb}^*V_{ts}\frac{e}{8\pi^2}. \tag{2.7}$$

At the next stage, K^* meson decays into K^0 and π^0 mesons through the strong interaction. The strong interaction conserves the C and P symmetries, then we can express the decay process by a common complex factor $f_1 \equiv A(K^{*0} \to K^0\pi^0) = A(\bar{K}^{*0} \to \bar{K}^0\pi^0)$ as shown in Fig. 3. Finally, we consider the process in which the K^0 meson goes to K_S or K_L. Here the indexes S, and L, express the "short," and "long" lifetimes, of two K mesons, respectively, and denote the amplitudes for $K^0 \to K_{S,L}$ and $\bar{K}^0 \to K_{S,L}$ as follows:

$$\begin{aligned} A(K^0 \to K_S) &= f_S, \qquad A(K^0 \to K_L) = f_L, \\ A(\bar{K}^0 \to K_S) &= f_S, \qquad A(\bar{K}^0 \to K_L) = -f_L. \end{aligned} \tag{2.8}$$

Then by denoting $F_S = f_1 f_S$ and $F_L = f_1 f_L$, the decay amplitudes for $B \to K_S\pi^0\gamma$ and $B \to K_L\pi^0\gamma$ can be expressed as follows:

$$\begin{aligned} A(B^0 \to K_S\pi^0\gamma_L) &= F_S A_L, \\ A(B^0 \to K_S\pi^0\gamma_R) &= F_S A_R, \\ A(\bar{B}^0 \to K_S\pi^0\gamma_L) &= F_S \bar{A}_L, \\ A(\bar{B}^0 \to K_S\pi^0\gamma_R) &= F_S \bar{A}_R, \end{aligned} \tag{2.9}$$

$$\begin{aligned} A(B^0 \to K_L\pi^0\gamma_L) &= F_L A_L, \\ A(B^0 \to K_L\pi^0\gamma_R) &= F_L A_R, \\ A(\bar{B}^0 \to K_L\pi^0\gamma_L) &= -F_L \bar{A}_L, \\ A(\bar{B}^0 \to K_L\pi^0\gamma_R) &= -F_L \bar{A}_R. \end{aligned} \tag{2.10}$$

Thus the time-dependent CP asymmetries become

$$\begin{aligned} A_{CP}(B^0 \to K_S\pi^0\gamma) &= \frac{\Gamma(\bar{B}^0(t) \to K_S\pi^0\gamma) - \Gamma(B^0(t) \to K_S\pi^0\gamma)}{\Gamma(\bar{B}^0(t) \to K_S\pi^0\gamma) + \Gamma(B^0(t) \to K_S\pi^0\gamma)} \\ &= \frac{Y}{X}\cos\Delta Mt + \frac{Z}{X}\sin\Delta Mt, \end{aligned} \tag{2.11}$$

$$\begin{aligned} A_{CP}(B^0 \to K_L\pi^0\gamma) &= \frac{\Gamma(\bar{B}^0(t) \to K_L\pi^0\gamma) - \Gamma(B^0(t) \to K_L\pi^0\gamma)}{\Gamma(\bar{B}^0(t) \to K_L\pi^0\gamma) + \Gamma(B^0(t) \to K_L\pi^0\gamma)} \\ &= \frac{Y}{X}\cos\Delta Mt - \frac{Z}{X}\sin\Delta Mt, \end{aligned} \tag{2.12}$$

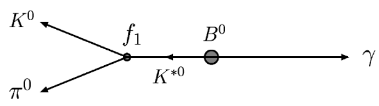

FIG. 3. The figure shows the $B^0 \to K^{*0}\gamma \to K^0\pi^0\gamma$ decay mode. The $K^{*0} \to K^0\pi^0$ process possesses the complex factor f_1 which is common in both $K^{*0} \to K^0\pi^0$ and $\bar{K}^{*0} \to \bar{K}^0\pi^0$ because the strong interaction conserves the C and P symmetries.

where we define

$$\begin{aligned} X &= |\bar{A}_L|^2 + |\bar{A}_R|^2 + |A_L|^2 + |A_R|^2, \\ Y &= |\bar{A}_L|^2 + |\bar{A}_R|^2 - (|A_L|^2 + |A_R|^2), \\ Z &= 2\,\mathrm{Im}[e^{-2i\phi_1}(\bar{A}_L A_L^* + \bar{A}_R A_R^*)], \end{aligned} \tag{2.13}$$

and we can see that the signs of the mixing-induced CP asymmetry between $B \to K_S\pi^0\gamma$ and $B \to K_L\pi^0\gamma$, which are proportional to $\sin\Delta Mt$, are opposite. The mixing-induced CP asymmetries are caused by the interferences between $\bar{A}_L$ and A_L, $\bar{A}_R$ and A_R.

The form factors in Eqs. (2.6) are related by C, P, and CP symmetries. We set the one form factor as the standard like $\langle K^{*0}\gamma_L|\bar{b}\sigma^{\mu\nu}(1+\gamma^5)sF_{\mu\nu}|B^0\rangle \equiv F_1$, the other form factors can be expressed as

$$\begin{aligned} &\langle K^{*0}\gamma_R|\bar{b}\sigma^{\mu\nu}(1-\gamma^5)sF_{\mu\nu}|B^0\rangle \\ &\quad = -\langle K^{*0}\gamma_L|P^\dagger P(\bar{b}\sigma^{\mu\nu}(1+\gamma^5)sF_{\mu\nu})P^\dagger P|B^0\rangle \\ &\quad = -F_1, \\ &\langle \bar{K}^{*0}\gamma_L|\bar{s}\sigma^{\mu\nu}(1+\gamma^5)bF_{\mu\nu}|\bar{B}^0\rangle \\ &\quad = \langle K^{*0}\gamma_L|C^\dagger C(\bar{b}\sigma^{\mu\nu}(1+\gamma^5)sF_{\mu\nu})C^\dagger C|B^0\rangle \\ &\quad = F_1 \\ &\langle \bar{K}^{*0}\gamma_R|\bar{s}\sigma^{\mu\nu}(1-\gamma^5)bF_{\mu\nu}|\bar{B}^0\rangle \\ &\quad = -\langle K^{*0}\gamma_L|CP^\dagger CP(\bar{b}\sigma^{\mu\nu}(1+\gamma^5)sF_{\mu\nu})CP^\dagger CP|B^0\rangle \\ &\quad = -F_1. \end{aligned} \tag{2.14}$$

Thus, Eqs. (2.6) can be expressed as

$$\begin{aligned} A_L &= m_s F F_1, \qquad A_R = -m_b F F_1, \\ \bar{A}_L &= m_b F^* F_1, \qquad \bar{A}_R = -m_s F^* F_1, \end{aligned} \tag{2.15}$$

and the mixing-induced CP asymmetries in Eqs. (2.11) and (2.12) become

$$S_{K_S\pi^0\gamma} = -S_{K_L\pi^0\gamma} = -2\frac{m_s}{m_b}\sin 2\phi_1. \tag{2.16}$$

That is, the mixing-induced CP asymmetries are predicted to be small within the SM roughly by the factor of m_s/m_b as pointed out by [12], because A_L and $\bar{A}_R$ are suppressed compared to A_R and $\bar{A}_L$.

However, in the near future, the mixing-induced CP asymmetry of $B \to K^*\gamma$ will become one of the most important tests for the SM, so it is very important to estimate the CP asymmetry more accurately by taking into account the small contributions compared to the dominant contribution caused in the $O_{7\gamma}$ operator. Cognizant of this point, we also consider chromomagnetic penguin (O_{8g}), the QCD annihilation ($O_3 \sim O_6$), u and c loop contributions, and also the long distance effects. Then we compute the mixing-induced CP asymmetry in $B \to K_S\pi^0\gamma$ and $B \to K_L\pi^0\gamma$ decays within the SM, and compare the experimental data given by [13–15].

III. FACTORIZATION FORMULA

The decay amplitudes can be factorized into scalar (M^S) and pseudoscalar (M^P) components as

$$M = (\epsilon_\gamma \cdot \epsilon_{K^*})M^S + i\epsilon_{\mu\nu+-}\epsilon_\gamma^\mu \epsilon_{K^*}^\nu M^P \quad (3.1)$$

where ϵ_γ, and ϵ_{K^*} are transverse polarization vectors for γ, and K^* mesons, respectively. In the $B \to K^*\gamma$ decay mode, the emitted photon is a real photon, so the chirality of the photon is constrained to be left handed or right handed, because the longitudinally polarized photon is forbidden by the gauge invariance. Then the polarization vector of the photon can be expressed as

$$\epsilon_\gamma{}^L = \left(0, 0, \frac{1}{\sqrt{2}}(1, i)\right), \qquad \epsilon_\gamma{}^R = \left(0, 0, \frac{1}{\sqrt{2}}(1, -i)\right), \quad (3.2)$$

and polarization of the K^* meson is uniquely determined by the helicity conservation of the spinless B meson decay as

$$\epsilon_{K^*}{}^R = \left(0, 0, \frac{1}{\sqrt{2}}(1, -i)\right), \qquad \epsilon_{K^*}{}^L = \left(0, 0, \frac{1}{\sqrt{2}}(1, i)\right). \quad (3.3)$$

The detailed expressions for the $B \to K^*\gamma$ decay amplitudes with the pQCD approach are in [11], then here we want to show the way how to divide the B meson amplitudes into the ones with left-handed or right-handed photon chiralities.

A. $O_{7\gamma}$ contribution

The decay amplitudes caused by $O_{7\gamma}$ components which are proportional to m_b as shown in Fig. 4 can be expressed as Eqs. (14) and (15) in [11]:

$$M_{7\gamma}^{S(a)}(m_b) = -M_{7\gamma}^{P(a)}(m_b) = r_b M_{7\gamma}^{S(a)} \quad (3.4)$$

$$M_{7\gamma}^{S(b)}(m_b) = -M_{7\gamma}^{P(b)}(m_b) = r_b M_{7\gamma}^{S(b)}, \quad (3.5)$$

where we define $r_q = m_q/M_B$. In this time, we distinctively express the quark mass m_b which comes from the $O_{7\gamma}$ operator from the meson mass M_B.

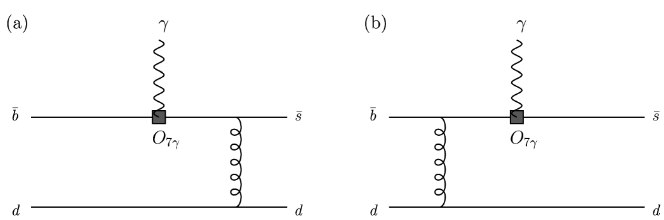

FIG. 4. The figure shows the $B^0 \to K^{*0}\gamma$ decay contribution caused by the $O_{7\gamma}$ operator. The photon is emitted from the operator, and the hard gluon exchange enables the fast moving K^* meson to form.

Here we want to concentrate on the characteristic relationship between the scalar and pseudoscalar components as $M_{7\gamma}^S(m_b) = -M_{7\gamma}^P(m_b)$. If we write down the decay amplitude as in the form of Eq. (3.1), we can factor out the common factor as

$$M = M_{7\gamma}^S(m_b)[(\epsilon_\gamma \cdot \epsilon_{K^*}) - i\epsilon_{\mu\nu+-}\epsilon_\gamma^\mu \epsilon_{K^*}^\nu]. \quad (3.6)$$

When we enter Eqs. (3.2) and (3.3) into Eq. (3.6), the combination ϵ_γ^R and $\epsilon_{K^*}^L$ only survives. That is, the chiralities of the photon and K^* meson are automatically determined, and in the B meson decay caused by the component of $O_{7\gamma}$ operator which is proportional to m_b, the emitted photon has necessary right-handed chirality.

The decay amplitude caused by the $O_{7\gamma}$ operator component which is proportional to m_s, on the other hand, becomes as follows:

$$M_{7\gamma}^{S(a)}(m_s) = M_{7\gamma}^{P(a)}(m_s) = -r_s M_{7\gamma}^{S(a)} \quad (3.7)$$

$$M_{7\gamma}^{S(b)}(m_s) = M_{7\gamma}^{P(b)}(m_s) = -r_s M_{7\gamma}^{S(b)}. \quad (3.8)$$

The characteristic relation $M_{7\gamma}^S(m_s) = M_{7\gamma}^P(m_s)$ implies that the combination ϵ_γ^L and $\epsilon_{K^*}^R$ only survives. It indicates that in the B meson decay caused by the component of the $O_{7\gamma}$ operator which is proportional to m_s, the photon has left-handed chirality.

Furthermore, we investigate the $\bar{B}$ meson decay. The amplitude for $\bar{B}$ meson decay can be extracted from the Hermite conjugate operator for the B meson decay:

$$\bar{M}_{7\gamma}^{S(a)}(m_b) = \bar{M}_{7\gamma}^{P(a)}(m_b) = -r_b \frac{\xi_t^*}{\xi_t} M_{7\gamma}^{S(a)} \quad (3.9)$$

$$\bar{M}_{7\gamma}^{S(b)}(m_b) = \bar{M}_{7\gamma}^{P(b)}(m_b) = -r_b \frac{\xi_t^*}{\xi_t} M_{7\gamma}^{S(b)} \quad (3.10)$$

$$\bar{M}_{7\gamma}^{S(a)}(m_s) = -\bar{M}_{7\gamma}^{P(a)}(m_s) = r_s \frac{\xi_t^*}{\xi_t} M_{7\gamma}^{S(a)} \quad (3.11)$$

$$\bar{M}_{7\gamma}^{S(b)}(m_s) = -\bar{M}_{7\gamma}^{P(b)}(m_s) = r_s \frac{\xi_t^*}{\xi_t} M_{7\gamma}^{S(b)}. \quad (3.12)$$

In $\bar{B}$ meson decay, the relations $\bar{M}_{7\gamma}^S(m_b) = \bar{M}_{7\gamma}^P(m_b)$ and $\bar{M}_{7\gamma}^S(m_s) = -\bar{M}_{7\gamma}^P(m_s)$ are satisfied, and they indicate that, in $\bar{B}$ meson decay, the photon chiralities are left handed and right handed, respectively.

We can summarize the B and $\bar{B}$ meson decay amplitudes A_R, A_L, $\bar{A}_R$, and $\bar{A}_L$ caused by the $O_{7\gamma}$ operator as follows:

$$A_{R_{7\gamma}} = (M_{7\gamma}^{S(a)}(m_b) + M_{7\gamma}^{S(b)}(m_b))[(\epsilon_\gamma \cdot \epsilon_{K^*}) - i\epsilon_{\mu\nu+-}\epsilon_\gamma^\mu \epsilon_{K^*}^\nu] \quad (3.13)$$

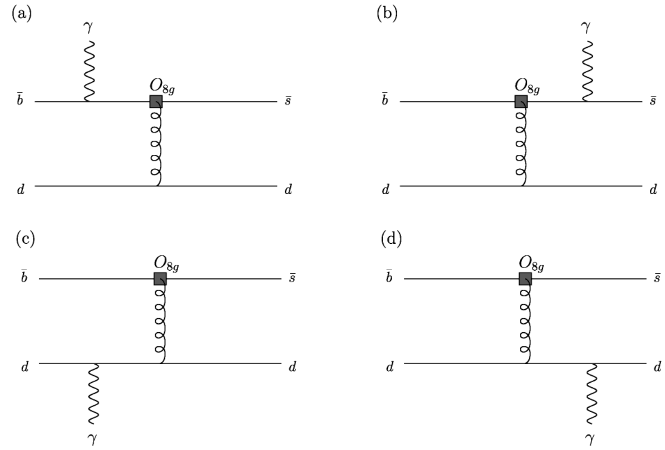

FIG. 5. Diagrams for the contribution of operator O_{8g}. The hard gluon is emitted from the operator and glued to the spectator quark, and photon is emitted by the bremsstrahlung from the external quark line.

$$A_{L_{7\gamma}} = (M_{7\gamma}^{S(a)}(m_s) + M_{7\gamma}^{A(b)}(m_s))[(\epsilon_\gamma \cdot \epsilon_{K^*}) + i\epsilon_{\mu\nu+-}\epsilon_\gamma^\mu \epsilon_{K^*}^\nu] \tag{3.14}$$

$$\bar{A}_{R_{7\gamma}} = -\frac{\xi_t^*}{\xi_t}(M_{7\gamma}^{S(a)}(m_s) + M_{7\gamma}^{S(b)}(m_s))[(\epsilon_\gamma \cdot \epsilon_{K^*}) - i\epsilon_{\mu\nu+-}\epsilon_\gamma^\mu \epsilon_{K^*}^\nu], \tag{3.15}$$

$$\bar{A}_{L_{7\gamma}} = -\frac{\xi_t^*}{\xi_t}(M_{7\gamma}^{S(a)}(m_b) + M_{7\gamma}^{S(b)}(m_b))[(\epsilon_\gamma \cdot \epsilon_{K^*}) + i\epsilon_{\mu\nu+-}\epsilon_\gamma^\mu \epsilon_{K^*}^\nu]. \tag{3.16}$$

From Eqs. (3.13), (3.14), (3.15), and (3.16), we can see that $A_{L_{7\gamma}}$ and $\bar{A}_{R_{7\gamma}}$ are certainly suppressed compared to $A_{R_{7\gamma}}$ and $\bar{A}_{L_{7\gamma}}$ by the factor of m_s/m_b within the SM. Furthermore, we can see the relationships $A_{R_{7\gamma}}/\xi_t = -\bar{A}_{L_{7\gamma}}/\xi_t^*$ and $A_{L_{7\gamma}}/\xi_t = -\bar{A}_{R_{7\gamma}}/\xi_t^*$ explicitly, which are discussed in Eqs. (2.15).

B. O_{8g} contribution

Next we concentrate on O_{8g} contributions as shown in Fig. 5. From Eqs. (19)–(22) in [11], we can see that the amplitudes from $M_{8g}^{(a)}(m_b)$ to $M_{8g}^{(c)}(m_b)$ satisfy the relationship $M_{8g}^S(m_b) = -M_{8g}^P(m_b)$, and they imply that the chirality of the photon from the B meson decay caused by the component of the O_{8g} operator which is proportional to m_b is right handed except for $M_{8g}^{(d)}(m_b)$. When we concentrate on the exceptional case $M_{8g}^{(d)}$, on the other hand, the twist-2 (leading) component for the K^* meson wave function $\phi_{K^*}^T$ also has an $M_{8g}^S(m_b) = -M_{8g}^P(m_b)$ relation. The origins to generate the difference between $M_{8g}^S(m_b)$ and $M_{8g}^P(m_b)$ are higher twist components, then the effect of the anomaly of the photon chirality should be small. If we divide $M_{8g}^{(d)}(m_b)$ components into right-handed and left-handed photon chirality amplitudes $M_{8g}^{(d)R}(m_b)$ and $M_{8g}^{(d)L}(m_b)$ by using the relationship as

$$\begin{aligned} M_{8g}^{(d)}(m_b) &= (\epsilon_\gamma \cdot \epsilon_{K^*})M_{8g}^{S(d)}(m_b) \\ &\quad + i\epsilon_{\mu\nu+-}\epsilon_\gamma^\mu \epsilon_{K^*}^\nu M_{8g}^{P(d)}(m_b) \\ &= M_{8g}^{S(d)R}(m_b)[(\epsilon_\gamma \cdot \epsilon_{K^*}) - i\epsilon_{\mu\nu+-}\epsilon_\gamma^\mu \epsilon_{K^*}^\nu] \\ &\quad + M_{8g}^{S(d)L}(m_b)[(\epsilon_\gamma \cdot \epsilon_{K^*}) + i\epsilon_{\mu\nu+-}\epsilon_\gamma^\mu \epsilon_{K^*}^\nu], \end{aligned} \tag{3.17}$$

they can be expressed as follows:

$$\begin{aligned} M_{8g}^{S(d)R}(m_b) &= -M_{8g}^{P(d)R}(m_b) \\ &= -F^{(0)}Q_d \xi_t r_b \int_0^1 dx_1 dx_2 \int b_1 d_1 b_2 db_2 \\ &\quad \times \phi_B(x_1, b_1)S_t(x_2)\alpha_s(t_8^d)e^{[-S_B(t_8^d)-S_{K^*}(t_8^d)]} \\ &\quad \times C_8(t_8^d)[3x_2 r_{K^*}[\phi_{K^*}^v(x_2) + \phi_{K^*}^a(x_2)] \\ &\quad + (2 + x_2 - x_1)\phi_{K^*}^T(x_2)] \\ &\quad \times H_8^{(d)}(\sqrt{|A_8'^2|}b_1, E_8 b_1, E_8 b_2), \end{aligned} \tag{3.18}$$

$$\begin{aligned} M_{8g}^{S(d)L}(m_b) &= M_{8g}^{P(d)L}(m_b) \\ &= -F^{(0)}Q_d \xi_t r_b \int_0^1 dx_1 dx_2 \int b_1 d_1 b_2 db_2 \\ &\quad \times \phi_B(x_1, b_1)S_t(x_2)\alpha_s(t_8^d)e^{[-S_B(t_8^d)-S_{K^*}(t_8^d)]} \\ &\quad \times C_8(t_8^d)3x_2 r_{K^*}[\phi_{K^*}^v(x_2) - \phi_{K^*}^a(x_2)] \\ &\quad \times H_8^{(d)}(\sqrt{|A_8'^2|}b_1, E_8 b_1, E_8 b_2). \end{aligned} \tag{3.19}$$

Then the decay amplitudes with left and right photon chirality can be expressed as follows:

$$\begin{aligned} A_{R_{8g}} &= (M_{8g}^{S(a)}(m_b) + M_{8g}^{S(b)}(m_b) + M_{8g}^{S(c)}(m_b) \\ &\quad + M_{8g}^{S(d)R}(m_b) + M_{8g}^{S(d)R}(m_s))[(\epsilon_\gamma \cdot \epsilon_{K^*}) \\ &\quad - i\epsilon_{\mu\nu+-}\epsilon_\gamma^\mu \epsilon_{K^*}^\nu], \end{aligned} \tag{3.20}$$

$$\begin{aligned} A_{L_{8g}} &= (M_{8g}^{S(a)}(m_s) + M_{8g}^{S(b)}(m_s) + M_{8g}^{S(c)}(m_s) \\ &\quad + M_{8g}^{S(d)L}(m_s) + M_{8g}^{S(d)L}(m_b))[(\epsilon_\gamma \cdot \epsilon_{K^*}) \\ &\quad + i\epsilon_{\mu\nu+-}\epsilon_\gamma^\mu \epsilon_{K^*}^\nu], \end{aligned} \tag{3.21}$$

$$\begin{aligned} \bar{A}_{R_{8g}} &= -\frac{\xi_t^*}{\xi_t}(M_{8g}^{S(a)}(m_s) + M_{8g}^{S(b)}(m_s) + M_{8g}^{S(c)}(m_s) \\ &\quad + M_{8g}^{S(d)L}(m_s) + M_{8g}^{S(d)L}(m_b))[(\epsilon_\gamma \cdot \epsilon_{K^*}) \\ &\quad - i\epsilon_{\mu\nu+-}\epsilon_\gamma^\mu \epsilon_{K^*}^\nu], \end{aligned} \tag{3.22}$$

$$\bar{A}_{L_{8g}} = -\frac{\xi_t^*}{\xi_t}(M_{8g}^{S(a)}(m_b) + M_{8g}^{S(b)}(m_b) + M_{8g}^{S(c)}(m_b) + M_{8g}^{S(d)R}(m_b) + M_{8g}^{S(d)R}(m_s))[(\epsilon_\gamma \cdot \epsilon_{K^*}) + i\epsilon_{\mu\nu+-}\epsilon_\gamma^\mu \epsilon_{K^*}^\nu]. \quad (3.23)$$

In this way, we can classify all the decay amplitudes in [11] into ones with left-handed or right-handed photon chiralities.

C. Loop contributions

1. Quark line photon emission

Here we mention about the charm and up loop quark contribution as in Fig. 6. In this case, the photon is emitted through the external quark lines. The detailed expressions for the decay amplitudes are shown from Eqs. (31)–(35) in [11], and $M_{1i}^{S(a)} = M_{1i}^{P(a)}$ means the photon chirality is left handed, and $M_{1i}^{S(b)} = -M_{1i}^{P(b)}$ and $M_{1i}^{S(c)} = -M_{1i}^{P(c)}$ indicate that the photon chirality is right handed. In the $M_{1i}^{(d)}$ case, we can divide the amplitudes into the ones with left-handed or right-handed photon chiralities by using Eq. (3.17):

$$\begin{aligned} M_{1i}^{S(d)R} &= -M_{1i}^{S(d)R} \\ &= \frac{Q_d}{2}F^{(0)}\xi_i \int_0^1 dx_1 dx_2 \int b_1 db_1 b_2 db_2 \\ &\quad \times e^{[-S_B(t_2^d)-S_{K^*}(t_2^d)]} C_2(t_2^d)\phi_B(x_1,b_1)\alpha_s(t_2^d)S_t(x_2) \\ &\quad \times H_2^{(d)}(\sqrt{|A_2'^2|}b_1, E_2 b_1, E_2 b_2)\left[G(m_i^2, -A_2'^2, t_2^d) - \frac{2}{3}\right] \\ &\quad \times [x_2 r_{K^*}(1+2x_2)[\phi_{K^*}^v(x_2) + \phi_{K^*}^a(x_2)] \\ &\quad + 3(x_2 - x_1)\phi_{K^*}^T(x_2)], \end{aligned} \quad (3.24)$$

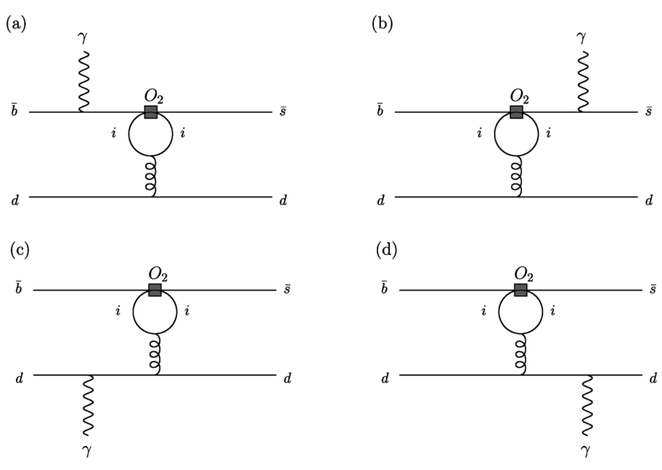

FIG. 6. Diagrams for $i = u$, c quark loop contributions inserted O_2 operator, with the photon emitted from the external quark line.

$$\begin{aligned} M_{1i}^{S(d)L} &= M_{1i}^{S(d)L} \\ &= \frac{Q_d}{2}F^{(0)}\xi_i \int_0^1 dx_1 dx_2 \int b_1 db_1 b_2 db_2 e^{[-S_B(t_2^d)-S_{K^*}(t_2^d)]} \\ &\quad \times C_2(t_2^d)\phi_B(x_1,b_1)\alpha_s(t_2^d)S_t(x_2) \\ &\quad \times H_2^{(d)}(\sqrt{|A_2'^2|}b_1, E_2 b_1, E_2 b_2)\left[G(m_i^2, -A_2'^2, t_2^d) - \frac{2}{3}\right] \\ &\quad \times x_2 r_{K^*}(2+x_2)[\phi_{K^*}^v(x_2) - \phi_{K^*}^a(x_2)]. \end{aligned} \quad (3.25)$$

Then the decay amplitudes with each photon chirality can be expressed as follows:

$$A_{R_{1i}} = (M_{1i}^{S(b)} + M_{1i}^{S(c)} + M_{1i}^{S(d)R})[(\epsilon_\gamma \cdot \epsilon_{K^*}) - i\epsilon_{\mu\nu+-}\epsilon_\gamma^\mu \epsilon_{K^*}^\nu], \quad (3.26)$$

$$A_{L_{1i}} = (M_{1i}^{S(a)} + M_{1i}^{S(d)L})[(\epsilon_\gamma \cdot \epsilon_{K^*}) + i\epsilon_{\mu\nu+-}\epsilon_\gamma^\mu \epsilon_{K^*}^\nu], \quad (3.27)$$

$$\bar{A}_{R_{1i}} = -\frac{\xi_i^*}{\xi_i}(M_{1i}^{S(a)} + M_{1i}^{S(d)L})[(\epsilon_\gamma \cdot \epsilon_{K^*}) - i\epsilon_{\mu\nu+-}\epsilon_\gamma^\mu \epsilon_{K^*}^\nu], \quad (3.28)$$

$$\bar{A}_{L_{1i}} = -\frac{\xi_i^*}{\xi_i}(M_{1i}^{S(b)} + M_{1i}^{S(c)} + M_{1i}^{S(d)R})[(\epsilon_\gamma \cdot \epsilon_{K^*}) + i\epsilon_{\mu\nu+-}\epsilon_\gamma^\mu \epsilon_{K^*}^\nu]. \quad (3.29)$$

2. Loop line photon emission

Next we consider the loop contributions in which the photon is emitted from the internal quark loop line as shown in Fig. 7. The explicit formulas for the decay amplitudes are Eqs. (42) and (43) in [11]. In this case, we can also divide the decay amplitudes into the ones with each photon chirality by using Eq. (3.17):

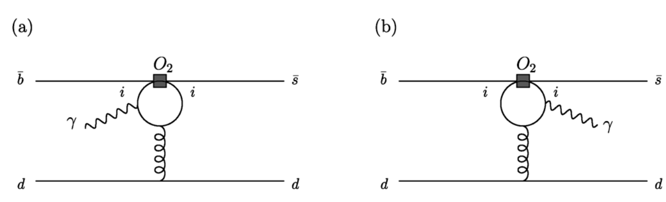

FIG. 7. Diagrams for $i = u$, c quark loop contributions inserted O_2 operator, with the photon emitted from the internal loop quark line.

$$M_{2i}^{SR} = -M_{2i}^{PR} = -\frac{4}{3}F^{(0)}\xi_i \int_0^1 dx \int_0^{1-x} dy \int_0^1 dx_1 dx_2 \times \int b_1 db_1 \phi_B(x_1, b_1) C_2(t_2)\alpha_s(t_2) e^{[-S_B(t_2)-S_{K^*}(t_2)]} \times \frac{1}{xyx_2 M_B^2 - m_i^2}[xyx_2[(1-x_2)r_{K^*}(\phi_{K^*}^v(x_2) + \phi_{K^*}^a(x_2)) - (1+2x_1)\phi_{K^*}^T(x_2)] + x(1-x)[x_2^2 r_{K^*}(\phi_{K^*}^v(x_2) + \phi_{K^*}^a(x_2)) + 3x_1x_2\phi_{K^*}^T(x_2)]]H_2(b_1A, b_1\sqrt{|B^2|}), \quad (3.30)$$

$$M_{2i}^{SL} = M_{2i}^{PL} = \frac{4}{3}F^{(0)}\xi_i \int_0^1 dx \int_0^{1-x} dy \int_0^1 dx_1 dx_2 \times \int b_1 db_1 \phi_B(x_1, b_1) C_2(t_2)\alpha_s(t_2) e^{[-S_B(t_2)-S_{K^*}(t_2)]} \times \frac{1}{xyx_2 M_B^2 - m_i^2} xyx_2^2 r_{K^*}[\phi_{K^*}^v(x_2) - \phi_{K^*}^a(x_2)] \times H_2(b_1A, b_1\sqrt{|B^2|}), \quad (3.31)$$

and we can summarize the decay amplitudes with each photon chirality as follows:

$$A_{R_{2i}} = M_{2i}^{SR}[(\epsilon_\gamma \cdot \epsilon_{K^*}) - i\epsilon_{\mu\nu+-}\epsilon_\gamma^\mu \epsilon_{K^*}^\nu], \quad (3.32)$$

$$A_{L_{2i}} = M_{2i}^{SL}[(\epsilon_\gamma \cdot \epsilon_{K^*}) + i\epsilon_{\mu\nu+-}\epsilon_\gamma^\mu \epsilon_{K^*}^\nu], \quad (3.33)$$

$$\bar{A}_{R_{2i}} = -\frac{\xi_i^*}{\xi_i} M_{2i}^{SL}[(\epsilon_\gamma \cdot \epsilon_{K^*}) - i\epsilon_{\mu\nu+-}\epsilon_\gamma^\mu \epsilon_{K^*}^\nu], \quad (3.34)$$

$$\bar{A}_{L_{2i}} = -\frac{\xi_i^*}{\xi_i} M_{2i}^{SR}[(\epsilon_\gamma \cdot \epsilon_{K^*}) + i\epsilon_{\mu\nu+-}\epsilon_\gamma^\mu \epsilon_{K^*}^\nu]. \quad (3.35)$$

D. Annihilation contributions

In this section, we want to discuss the annihilation contributions caused by QCD penguin operators from O_3 to O_6 shown in Fig. 8. In the neutral mode, the tree annihilations caused by O_1, O_2 do not exist. O_3, O_4, and O_5, O_6 operators have $(V-A)(V-A)$, and $(V-A)(V+A)$ vertices, respectively, and we define $a_4(t) = C_4(t) + C_3(t)/3$, $a_6(t) = C_6(t) + C_5(t)/3$. From Eqs. (55)–(62) in [11], we can see that $M_4^{(a)}$ has left-handed photon chirality, and $M_4^{(c)}$, $M_6^{(b)}$, and $M_6^{(d)}$ have right-handed photon chirality. Furthermore, we can divide $M_4^{(b)}$ and $M_4^{(d)}$ into the ones with left- or right-handed photon chiralities as follows:

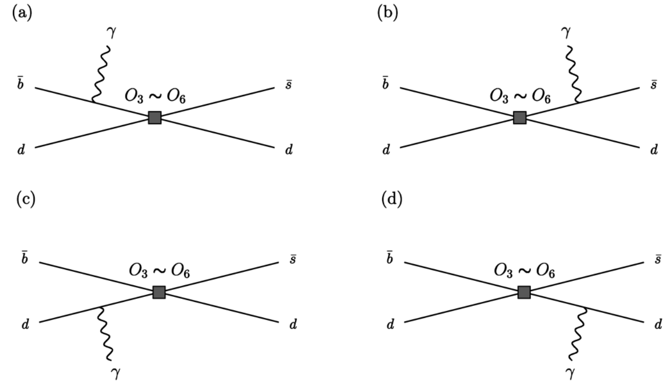

FIG. 8. Annihilation diagrams with QCD penguin operators O_i inserted.

$$M_4^{S(b)R} = -M_4^{P(b)R} = F^{(0)}\frac{3\sqrt{6}Q_s f_B \pi}{4M_B^2} r_{K^*}\xi_t \int_0^1 dx_2 \times \int b_2 db_2 a_4(t_a^b) S_t(x_2) e^{[-S_{K^*}(t_a^b)]} i\frac{\pi}{2} H_0^{(1)}(b_2B_a) \times [\phi_{K^*}^v(x_2) + \phi_{K^*}^a(x_2)], \quad (3.36)$$

$$M_4^{S(b)L} = M_4^{P(b)L} = F^{(0)}\frac{3\sqrt{6}Q_s f_B \pi}{4M_B^2} r_{K^*}\xi_t \int_0^1 dx_2 \times \int b_2 db_2 a_4(t_a^b) S_t(x_2) e^{[-S_{K^*}(t_a^b)]} i\frac{\pi}{2} \times H_0^{(1)}(b_2B_a)(1-x_2)[\phi_{K^*}^v(x_2) + \phi_{K^*}^a(x_2)]. \quad (3.37)$$

$$M_4^{S(d)R} = -M_4^{P(d)R} = -F^{(0)}\frac{3\sqrt{6}Q_s f_B \pi}{4M_B^2} r_{K^*}\xi_t \int_0^1 dx_2 \times \int b_2 db_2 a_4(t_a^b) S_t(x_2) e^{[-S_{K^*}(t_a^b)]} i\frac{\pi}{2} \times H_0^{(1)}(b_2B_a)x_2[\phi_{K^*}^v(x_2) + \phi_{K^*}^a(x_2)], \quad (3.38)$$

$$M_4^{S(d)L} = M_4^{P(d)L} = -F^{(0)}\frac{3\sqrt{6}Q_s f_B \pi}{4M_B^2} r_{K^*}\xi_t \int_0^1 dx_2 \times \int b_2 db_2 a_4(t_a^b) S_t(x_2) e^{[-S_{K^*}(t_a^b)]} i\frac{\pi}{2} \times H_0^{(1)}(b_2B_a)[\phi_{K^*}^v(x_2) - \phi_{K^*}^a(x_2)]. \quad (3.39)$$

Then we can summarize the decay amplitudes with each photon chirality as follows:

$$A_{R_4} = (M_4^{S(b)R} + M_4^{S(c)} + M_4^{S(d)R})[(\epsilon_\gamma \cdot \epsilon_{K^*}) - i\epsilon_{\mu\nu+-}\epsilon_\gamma^\mu \epsilon_{K^*}^\nu], \tag{3.40}$$

$$A_{L_4} = (M_4^{S(a)} + M_4^{S(b)L} + M_4^{S(d)L})[(\epsilon_\gamma \cdot \epsilon_{K^*}) + i\epsilon_{\mu\nu+-}\epsilon_\gamma^\mu \epsilon_{K^*}^\nu], \tag{3.41}$$

$$\bar{A}_{R_4} = -\frac{\xi_t^*}{\xi_t}(M_4^{S(a)} + M_4^{S(b)L} + M_4^{S(d)L})[(\epsilon_\gamma \cdot \epsilon_{K^*}) - i\epsilon_{\mu\nu+-}\epsilon_\gamma^\mu \epsilon_{K^*}^\nu], \tag{3.42}$$

$$\bar{A}_{L_4} = -\frac{\xi_t^*}{\xi_t}(M_4^{S(b)R} + M_4^{S(c)} + M_4^{S(d)R})[(\epsilon_\gamma \cdot \epsilon_{K^*}) + i\epsilon_{\mu\nu+-}\epsilon_\gamma^\mu \epsilon_{K^*}^\nu], \tag{3.43}$$

$$A_{R_6} = (M_6^{S(b)} + M_6^{S(d)})[(\epsilon_\gamma \cdot \epsilon_{K^*}) - i\epsilon_{\mu\nu+-}\epsilon_\gamma^\mu \epsilon_{K^*}^\nu], \tag{3.44}$$

$$A_{L_6} = \bar{A}_{R_6} = 0, \tag{3.45}$$

$$\bar{A}_{L_6} = -\frac{\xi_t^*}{\xi_t}(M_6^{S(b)} + M_6^{S(d)})[(\epsilon_\gamma \cdot \epsilon_{K^*}) + i\epsilon_{\mu\nu+-}\epsilon_\gamma^\mu \epsilon_{K^*}^\nu]. \tag{3.46}$$

E. Long distance contributions to the photon quark coupling

Here we want to discuss the long distance contributions. In order to examine the SM or search for new physics indirectly by comparing the experimental data with the values predicted within the SM, we have to take into account these long distance effects: $B \to K^*(\psi, \rho, \omega) \to K^*\gamma$ (Fig. 9). If we use the vector-meson dominance, the $B \to K^*\gamma$ decay amplitude can be expressed as inserting the complete set of possible intermediate vector meson states like

$$\langle K^*\gamma|H_{\rm eff}|B\rangle = \sum_V \langle\gamma|A_\nu J_{\rm em}^\nu|V\rangle \frac{-i}{q_V^2 - m_V^2}\langle VK^*|H_{\rm eff}|B\rangle, \tag{3.47}$$

where $V = \psi,\ \rho,\ \omega$. Now we concretely consider $B \to K^*\psi \to K^*\gamma$. Four diagrams contribute to the hadronic matrix element of $\langle K^*\psi|H_{\rm eff}|B\rangle$ (see Fig. 10), and first of all, we consider the leading contributions: the factorizable ones shown in Figs. 10(a) and 10(b).

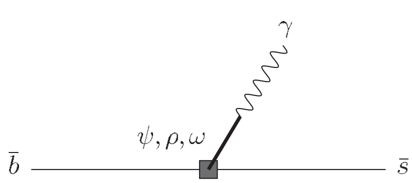

FIG. 9. Vector-meson-dominance contributions mediated by ψ, ρ, ω.

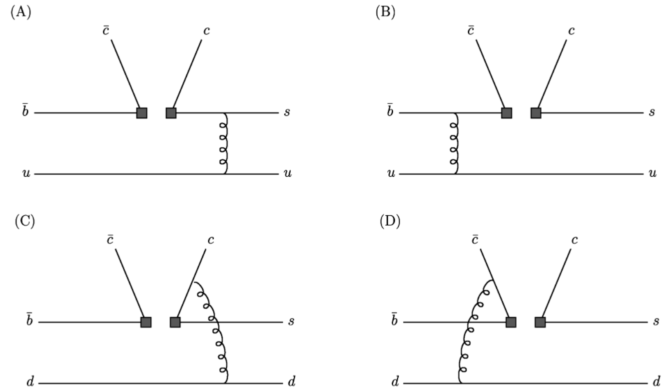

FIG. 10. (A), (B) are factorizable and (C), (D) are nonfactorizable contributions to the hadronic matrix element for $\langle K^*\psi|H_{\rm eff}|B\rangle$.

1. Factorizable contribution

The detailed explanation for the derivation of the factorizable amplitudes and explicit formulas is from Eqs. (77)–(79) in [11]. The momentum of the photon $q^2 = 0$ is smaller than the threshold mass $4m_u^2$, then the imaginary part from the decay width in the propagator of the ρ meson should not be generated. The long distance contribution mediated by the ρ meson is much smaller than the u quark loop contributions, the change does not effect the final numerical results. We can see that $M_{LD}^{(A)}$ has right-handed photon chirality, and for $M_{LD}^{(B)}$, it is also possible to divide it into the ones with left- or right-handed photon chiralities as mentioned above, and the results become as follows:

$$\begin{aligned} M_{LD}^{S(B)R} = -M_{LD}^{P(B)R} = \frac{8\pi^2}{M_B^2}F^{(0)}\int_0^1 dx_1 dx_2 \int b_1 db_1 b_2 db_2 \\ \times \phi_B(x_1, b_1)S_t(x_2)\alpha_s(t_7^b)e^{[-S_B(t_7^b)-S_{K^*}(t_7^b)]}a_1(t_7^b) \\ \times H_7^{(b)}(A_7 b_1, C_7 b_1, C_7 b_2)[r_{K^*}\phi_{K^*}^v(x_2) + \phi_{K^*}^T(x_2) \\ + r_{K^*}\phi_{K^*}^a(x_2)]\bigg(\xi_c \frac{2\kappa g_\psi(m_\psi^2)^2}{3} \\ + \xi_u\bigg[\frac{g_\omega(m_\omega^2)^2}{6} + \frac{g_\rho(m_\rho^2)^2}{2}\bigg]\bigg), \end{aligned} \tag{3.48}$$

$$\begin{aligned} M_{LD}^{S(B)L} = M_{LD}^{P(B)L} = \frac{8\pi^2}{M_B^2}F^{(0)}\int_0^1 dx_1 dx_2 \int b_1 db_1 b_2 db_2 \\ \times \phi_B(x_1, b_1)S_t(x_2)\alpha_s(t_7^b)e^{[-S_B(t_7^b)-S_{K^*}(t_7^b)]}a_1(t_7^b) \\ \times H_7^{(b)}(A_7 b_1, C_7 b_1, C_7 b_2)r_{K^*}(1 + x_2)[\phi_{K^*}^v(x_2) \\ \times -\phi_{K^*}^a(x_2)]\bigg(\xi_c \frac{2\kappa g_\psi(m_\psi^2)^2}{3} \\ + \xi_u\bigg[\frac{g_\omega(m_\omega^2)^2}{6} + \frac{g_\rho(m_\rho^2)^2}{2}\bigg]\bigg), \end{aligned} \tag{3.49}$$

$$A_{R_{LD}} = (M_{LD}^{S(A)} + M_{LD}^{S(B)R})[(\epsilon_\gamma \cdot \epsilon_{K^*}) - i\epsilon_{\mu\nu+-}\epsilon_\gamma^\mu \epsilon_{K^*}^\nu], \tag{3.50}$$

$$A_{L_{LD}} = M_{LD}^{S(B)L}[(\epsilon_\gamma \cdot \epsilon_{K^*}) + i\epsilon_{\mu\nu+-}\epsilon_\gamma^\mu \epsilon_{K^*}^\nu], \tag{3.51}$$

$$\bar{A}_{R_{LD}} = -\frac{\xi_i^*}{\xi} M_{LD}^{S(B)L}[(\epsilon_\gamma \cdot \epsilon_{K^*}) - i\epsilon_{\mu\nu+-}\epsilon_\gamma^\mu \epsilon_{K^*}^\nu], \tag{3.52}$$

$$\bar{A}_{L_{LD}} = -\frac{\xi_i^*}{\xi}(M_{LD}^{S(A)} + M_{LD}^{S(B)R})[(\epsilon_\gamma \cdot \epsilon_{K^*}) + i\epsilon_{\mu\nu+-}\epsilon_\gamma^\mu \epsilon_{K^*}^\nu]. \tag{3.53}$$

2. *Nonfactorizable contribution*

Next we consider the nonfactorizable long distance contributions as in Figs. 10(c) and 10(d). In order to estimate the effect to the total mixing-induced *CP* asymmetry, we roughly estimate the degree of nonfactorizable long distance contribution to the factorizable long distance contribution. We have already known that the theoretical computation which is estimated by including only the factorizable contribution and experimental data for the transversely polarized branching ratio in $B \to J/\psi K^*$ decay mode do not agree with each other [11]. If we assume that the difference between the experimental value and theoretical prediction is due to the nonfactorizable amplitude, we expect that it amounts to about 40% contribution to the factorizable amplitude. We include the nonfactorizable contribution as the free parameter which satisfies the condition such that its contribution amounts to about 40% to the factorizable one, and we numerically compute the effect to the mixing-induced *CP* asymmetry as show in Sec. IV.

IV. NUMERICAL RESULTS

We want to show the numerical analysis in this section. In the evaluation of the various form factors and amplitudes, we adopt $G_F = 1.16639 \times 10^{-5}$ GeV^{-2}, leading order strong coupling α_s defined at the flavor number $n_f = 4$, the decay constants $f_B = 190$ MeV, $f_{K^*} = 226$ MeV, and $f_{K^*}^T = 185$ MeV, the masses $M_B = 5.28$ GeV, $M_{K^*} = 0.892$ GeV $m_b = 4.8$ GeV, $m_c = 1.2$ GeV, and $m_s = 0.12$ GeV [20], and the meson lifetime $\tau_{B^0} = 1.542$ ps. Furthermore we used the leading order Wilson coefficients [19] and we take the K^*, ρ, and ω meson wave functions up to twist-3.

In order to compute the mixing-induced *CP* asymmetry, we clarify the theoretical error for it.

(1) First if we change the meson wave function parameter in the range $\omega_B = (0.40 \pm 0.04)$ GeV, the uncertainty of the mixing-induced *CP* asymmetry amounts to about 10%. Furthermore, the uncertainties from the quark mass amount to about 20%. Then the error from the input parameters is about 20%.

(2) We can expect that the uncertainty from the higher order effects should be largely canceled because we take the ratio in the computation of the asymmetry.

(3) About the error from the Cabibbo-Kobayashi-Maskawa (CKM) parameters, we change the $\bar{\rho}$, $\bar{\eta}$ parameters in the range $\bar{\rho} = \rho(1 - \lambda^2/2) = 0.20 \pm 0.09$ and $\bar{\eta} = \eta(1 - \lambda^2/2) = 0.33 \pm 0.05$ [21], and numerically estimate how the physical quantities are affected by the change of parameters. The result is that about 30% error is generated by the uncertainty for the CKM parameters.

(4) Furthermore, we introduce the nonfactorizable long distance contribution as mentioned in Sec. III E 2, and it can generates about 30% error for the asymmetry.

(5) Finally, we introduce 100% hadronic uncertainty for the u quark loop, and the asymmetry changes about 10%. In summary, the total theoretical error amounts to about 50% for the mixing-induced *CP* asymmetry.

Then the numerical results for the mixing-induced *CP* asymmetries in $B \to K_S\pi^0\gamma$ and $B \to K_L\pi^0\gamma$ like Eqs. (2.11) and (2.12) which are caused by $O_{7\gamma}$, O_{8g}, c, and u quark loop contributions, QCD annihilations, and the factorizable and nonfactorizable long distance contributions become as follows:

$$S_{K_S\pi^0\gamma} = -S_{K_L\pi^0\gamma} = -(3.5 \pm 1.7) \times 10^{-2}. \tag{4.1}$$

V. CONCLUSION

In this paper, we compute the mixing-induced *CP* asymmetry in the $B \to K^*\gamma$ decay mode with perturbative QCD approach by including also the small contributions except for the dominant $O_{7\gamma}$ amplitude. Within the SM, we can roughly estimate the asymmetry as $S_{K_S\pi^0\gamma}^{\rm SM} \simeq -2\frac{m_s}{m_b} \times \sin2\phi_1 = -(2.7 \pm 0.9) \times 10^{-2}$, when we change the CKM parameters as $\bar{\rho} = 0.20 \pm 0.09$ and $\bar{\eta} = 0.33 \pm 0.05$. If we compute the asymmetry by taking into account for only $O_{7\gamma}$, our computation becomes $S_{K_S\pi^0\gamma} = -(2.7 \pm 0.9) \times 10^{-2}$. Comparing the above two values, we can check that our computation goes well, and contributions except for $O_{7\gamma}$ generate about 15% asymmetry. Then we investigated what contribution except for $O_{7\gamma}$ makes a difference from Eq. (4.1). If we neglect the QCD annihilation contributions, the asymmetry becomes as $S_{K_S\pi^0\gamma} = -(3.8 \pm 1.7) \times 10^{-2}$, by abandoning all the long distance contributions, $S_{K_S\pi^0\gamma} = -(3.4 \pm 1.3) \times 10^{-2}$, and we discard the u and c quark loop contributions $S_{K_S\pi^0\gamma} = -(3.0 \pm 1.4) \times 10^{-2}$ and $S_{K_S\pi^0\gamma} = -(3.3 \pm 1.6) \times 10^{-2}$, respectively. From the above consideration, the most effective contribution which generates the difference from the prediction with only $O_{7\gamma}$ amplitude is the u quark loop contribution, because the amplitude with left-handed photon chirality for B^0 meson decay in Eq. (3.31) can interfere with the right-handed photon chirality as mentioned in [22,23].

The experimental data for the mixing-induced *CP* asymmetry in $B \to K_s \pi^0 \gamma$ are given by Belle and *BABAR* as follows [13–15]:

$$S^{\mathrm{ex}}_{K^* \gamma \to K_S \pi^0 \gamma} = \begin{cases} -0.79^{+0.63}_{-0.50} \pm 0.10 & [\mathrm{Belle}], \\ -0.21 \pm 0.40 \pm 0.05 & [BABAR]. \end{cases} \tag{5.1}$$

Comparing our prediction in Eq. (4.1) with the experimental data in Eqs. (5.1), we can see that our theoretical prediction is included in the range of the experimental data. Furthermore, the time-dependent oscillations in $B \to K_S \pi^0 \gamma$ do not depend on the resonance structure; whether the $K_S \pi^0 \gamma$ final state comes from K^* or not [24]. The fact will be helpful experimentally to accumulate higher statistics. Then we look forward to the improvement of the experimental error in the near future and also for the Super B factory when it is built.

ACKNOWLEDGMENTS

We acknowledge helpful and valuable suggestions, discussions, and advices with Professor Amarjit Soni and Professor Hsiang-nan Li. A. I. S acknowledges support from JSPS Grant No. C-17540248.

[1] M. Kobayashi and T. Maskawa, Prog. Theor. Phys. **49**, 652 (1973).
[2] K. Abe *et al.* (Belle Collaboration), hep-ex/0308036.
[3] G. Raven, sin(2β)*: Status and Prospects*, eConf C0304052, WG417 (2003).
[4] K. Abe *et al.* (Belle Collaboration), Phys. Rev. Lett. **95**, 101801 (2005).
[5] A. Bevan (*BABAR* Collaboration), hep-ex/0411090.
[6] K. Abe *et al.* (Belle Collaboration), hep-ex/0411049.
[7] B. Aubert *et al.* (*BABAR* Collaboration), Phys. Rev. Lett. **95**, 121802 (2005).
[8] M. Nakao *et al.* (BELLE Colaboration), Phys. Rev. D **69**, 112001 (2004).
[9] B. Aubert *et al.* (*BABAR* Collaboration), Phys. Rev. D **70**, 112006 (2004).
[10] H. n. Li and G. L. Lin, Phys. Rev. D **60**, 054001 (1999).
[11] Y. Y. Keum, M. Matsumori, and A. I. Sanda, Phys. Rev. D **72**, 014013 (2005).
[12] D. Atwood, M. Gronau, and A. Soni, Phys. Rev. Lett. **79**, 185 (1997).
[13] Y. Ushiroda *et al.*, Phys. Rev. Lett. **94**, 231601 (2005).
[14] K. Abe *et al.* (BELLE Colaboration), hep-ex/0409049.
[15] B. Aubert *et al.* (*BABAR* Collaboration), Phys. Rev. D **72**, 051103 (2005).
[16] A. B. Carter and A. I. Sanda, Phys. Rev. Lett. **45**, 952 (1980).
[17] A. B. Carter and A. I. Sanda, Phys. Rev. D **23**, 1567 (1981).
[18] I. I. Y. Bigi and A. I. Sanda, Nucl. Phys. **B193**, 85 (1981).
[19] G. Buchalla, A. J. Buras, and M. E. Lautenbacher, Rev. Mod. Phys. **68**, 1125 (1996).
[20] M. Gockeler *et al.* (QCDSF Collaboration), Proc. Sci., LAT2005 (2005) 078 [hep-lat/0509159].
[21] S. Eidelman *et al.* (Particle Data Group), Phys. Lett. B **592**, 1 (2004).
[22] B. Grinstein, Y. Grossman, Z. Ligeti, and D. Pirjol, Phys. Rev. D **71**, 011504 (2005).
[23] B. Grinstein and D. Pirjol, Phys. Rev. D **73**, 014013 (2006).
[24] D. Atwood, T. Gershon, M. Hazumi, and A. Soni, Phys. Rev. D **71**, 076003 (2005).